Supplementary Information for:

A robotic platform for fluidically-linked human body-on-chips experimentation

Richard Novak[1*], Miles Ingram[1*], Susan Clauson[1*], Debarun Das[2*], Aaron Delahanty[1*], Anna Herland[1,*], Ben M. Maoz[1,3*], Sauveur S. F. Jeanty[1*+], Mahadevabharath R. Somayaji[2*], Morgan Burt[1], Elizabeth Calamari[1], Angeliki Chalkiadaki[1], Alexander Cho[2], Youngjae Choe[1], David Benson Chou[1,4], Michael Cronce[1], Stephanie Dauth[1,3], Toni Divic[1], Jose Fernandez-Alcon[1+], Thomas Ferrante[1], John Ferrier[1,3], Edward A. FitzGerald[1], Rachel Fleming[1], Sasan Jalili-Firoozinezhad[1,5], Thomas Grevesse[1,3], Josue A. Goss[1,3], Tiama Hamkins-Indik[1], Olivier Henry[1], Chris Hinojosa[1+], Tessa Huffstater[1], Kyung-Jin Jang[1+], Ville Kujala[1,3+], Lian Leng[1+], Robert Mannix[1,6], Yuka Milton[1], Janna Nawroth[1,3+], Bret A. Nestor[1], Carlos F. Ng[1], Blakely O'Connor[1,3], Tae-Eun Park[1], Henry Sanchez[1], Josiah Sliz[1+], Alexandra Sontheimer-Phelps[1,7], Ben Swenor[1], Guy Thompson II[1+], George J. Touloumes[1,3], Zachary Tranchemontagne[1], Norman Wen[1+], Moran Yadid[1,3], Anthony Bahinski[1,8], Geraldine A. Hamilton[1+], Daniel Levner[1,+], Oren Levy[1], Andrzej Przekwas[2], Rachelle Prantil-Baun[1], Kevin K. Parker[1,3], and Donald E. Ingber[1,3,6]

[1]Wyss Institute for Biologically Inspired Engineering at Harvard University, Boston, MA 02115, USA; [2]CFD Research Corporation, Huntsville, AL, USA 35806; [3]Harvard John A. Paulson School of Engineering and Applied Sciences, Harvard University, Cambridge, MA 02138, USA; [4]Department of Pathology, Massachusetts General Hospital, Boston, MA 02115, USA; [5]Department of Bioengineering and iBB - Institute for Bioengineering and Biosciences, Instituto Superior Técnico, Universidade de Lisboa, Lisboa, Portugal; [6]Vascular Biology Program and Department of Surgery, Boston Children's Hospital and Harvard Medical School, Boston, MA 02115, USA; [7]Department of Biology, University of Freiburg, Freiburg, Germany; [8]GlaxoSmithKline, 1250 S. Collegeville Rd., Collegeville, PA 19426, USA;

[*] Authors contributed equally

[+] Current address: Emulate, Inc., 27 Drydock Avenue, Boston, MA 02210, USA

Stage Calibration

The deck layout exists in three spaces: the physical layout, the CAD assembly and the web-based GUI. The calibration protocol developed here relates the positional error between the physical and CAD layouts. The measured positional errors can then be used to calculate linear scaling and offset values that, when applied in the web-based GUI, significantly reduce alignment error between the liquid handler and the individual deck components. A given x,y,z coordinate as described by the CAD layout is calibrated to the physical layout by multiplying the spatial coordinates by a calibration matrix and adding an offset matrix. A schematic of this calibration is shown in **Fig. 2~~3~~b**. In a perfectly aligned system, the calibration matrix would simply be an identity matrix (Equation 1) and all offset values would be zero (Equation 2). In order to use this calibration procedure, robot alignment error must be determined by installing four precision ground post subassemblies (Thorlabs P series 1.5" diameter post, MiSUMi M6 10mm diameter locating pin) used as calibration references and a ruby-probe tip (Renishaw 1mm ball end 10 mm length, M4 thread) attached to the end of the liquid handler with a custom tapped 20 mm long spacer (M4 female to ¼-28 female). Two matrices are generated; matrix ‘P’, the theoretical, CAD-based, distance between the four measurement references (equation 3), and matrix ‘Q’, the physically measured distance between the four calibration references (equation 4). The web-based GUI features an interactive aid to complete the measurement process; upon completion, the calibration posts are removed. The process of determining the calibration and offset matrix is shown in equations 5 and 6, respectively. Once the M and O matrices have been determined, they are permanently stored within the client code and are applied to all motion system coordinates as directed by the web-based GUI. The calibration procedure is run when the system is assembled and re-calibrated upon software re-install, if any major changes are made to the deck layout, or at regularly scheduled maintenance intervals.

$$M = \begin{bmatrix} 1 & 0 & 0 \\ 0 & 1 & 0 \\ 0 & 0 & 1 \end{bmatrix} \quad \text{[Eq. 1]}$$

$$O = \begin{bmatrix} 0 & 0 & 0 \end{bmatrix} \quad \text{[Eq. 2]}$$

$$P = \begin{bmatrix} (B_{x1} - A_{x1}) & (B_{y1} - A_{y1}) & (B_{z1} - A_{z1}) \\ (C_{x1} - A_{x1}) & (C_{y1} - A_{y1}) & (C_{z1} - A_{z1}) \\ (D_{x1} - A_{x1}) & (D_{y1} - A_{y1}) & (D_{z1} - A_{z1}) \end{bmatrix} \quad \text{[Eq. 3]}$$

$$Q = \begin{bmatrix} (B_{x2} - A_{x2}) & (B_{y2} - A_{y2}) & (B_{z2} - A_{z2}) \\ (C_{x2} - A_{x2}) & (C_{y2} - A_{y2}) & (C_{z2} - A_{z2}) \\ (D_{x2} - A_{x2}) & (D_{y2} - A_{y2}) & (D_{z2} - A_{z2}) \end{bmatrix} \quad \text{[Eq. 4]}$$

$$M = [Q][P]^{-1} \quad \text{[Eq. 5]}$$

$$\begin{bmatrix} O_x & O_y & O_z \end{bmatrix} = \begin{bmatrix} A_{x2} & A_{y2} & A_{z2} \end{bmatrix} - \begin{bmatrix} A_{x1} & A_{y1} & A_{z1} \end{bmatrix} [M] \quad \text{[Eq. 6]}$$

SI Table 1. Organ Chip types and associated properties of the microfluidic features.

Organ Chip	Membrane	Channel Width (mm)	Apical Channel Height (mm)	Basal Channel Height (mm)	Channel Length (mm)
Gut	PDMS 7 µm pores	1	1	0.2	91
Liver	PDMS 7 µm pores	1	1	0.2	24
Kidney	PET 0.4 µm pores	1	0.1	0.1	24
Heart	PC 5 µm pores	2.5	0.25	1.2	25
Lung	PDMS 7µm pores	1	1	0.2	24
Skin	PDMS 7µm pores	5.5 (apical) 1 (basal)	5	0.3	24
BBB	PET 0.4 µm pores	1	1	0.2	24
Brain	PC 5 µm pores	2.5	0.1	1.2	25

PDMS: poly (dimethyl siloxane); PET: polyester terephthalate; PC: polycarbonate

SI Table 2 – Cell culture parameters

Organ	Chip Type	ECM Coating	Apical		Basal	
			Cell Type	Seeding Density	Cell Type	Seeding Density
Gut	Long Tall Channel, Stretchable, PDMS Membrane	Matrigel & Collagen I	Caco2 BBE	100,000 cells/cm^2	HUVEC	100,000 cells/cm^2
Liver	Standard Tall Channel, Stretchable, PDMS Membrane	Collagen I	Primary Human Hepatocytes	250,000 cells/cm^2	LSEC	100,000 cells/cm^2
Kidney	Standard tall channel, PET membrane	Collagen IV & Laminin	Human Renal Proximal Tubule	120,000 cells/cm^2	Human Glomerular Microvascular Endothelial	100,000 cells/cm^2
Heart	Dual channel PC, PET Membrane	Fibronectin	Human iPSC Cardiomyocytes (Cor4U, Axiogenesis)	200,000 cell/cm^2	HUVEC	100,000 cells/cm^2
Lung	Standard Tall Channel, Stretchable, PDMS Membrane	Fibronectin & Collagen I	A549 Human Lung Carcinoma Cell Line	200,000 cells/cm^2	HUVEC	60,000 cells/cm^2
BBB	Standard tall channel, PET membrane	Collagen IV & Fibronectin	Primary Human Astrocytes	70,000 cells/cm^2	Primary Human Brain Microvascular Endothelial	90,000 cells/cm^2
			Primary Human Pericytes	30,000 cells/cm^2		
Brain	Dual channel PC, PET Membrane	PDL & Laminin	Human Hippocampal Neural Stem Cells (hNSCs)	100,000 cells/cm^2	N/A	
Skin	Oval Open-top, Stretchable, PDMS Membrane	Fibronectin & Collagen I	Human Primary Adult Dermal Fibroblasts	82,000 cells/cm^2	Human Primary Dermal Microvascular Endothelial	100,000 cells/cm^2
			Human Primary Neonatal Epidermal Keratinocytes	800,000 cells/cm^2		

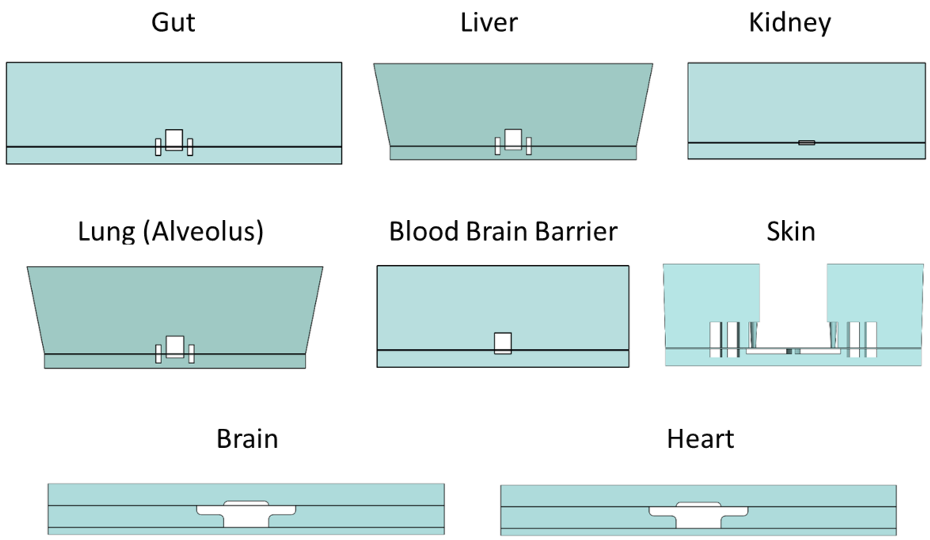

Supplementary Figure S1. Cross sectional views of Organ Chip CAD for all 8 Organ Chips used in this study. In all chips, two parallel fluidic channels are separated by a porous semi-permeable membrane.

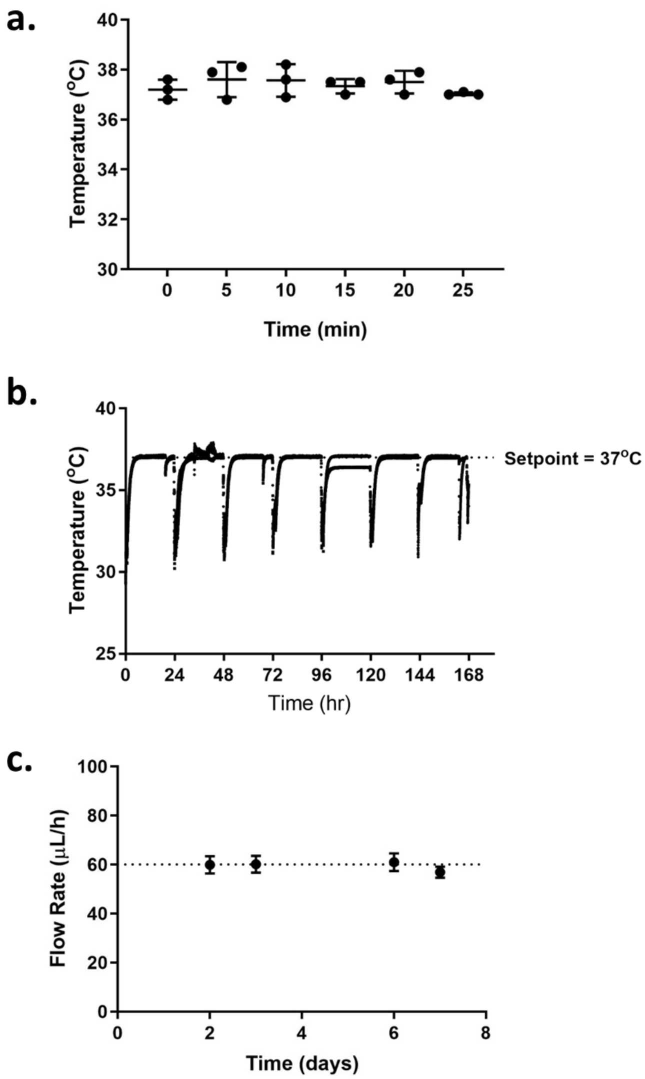

Supplementary Figure S2. Characterization of Interrogator operation with respect to temperature during continuous fluid handling (**A**) indicates minimal impact of electronics on incubator thermal stability. Thermal stability was also not affected over the course of an Organ Chip linking study (**B**). Drops in temperature indicate incubator door opening to exchange plates and reagents. The peristaltic pump flow rate (**C**) remained within 10% of the nominal setpoint for at least one week of operation.

Formatted: Font: Bold

Formatted: Font: Bold

Formatted: Font: Bold

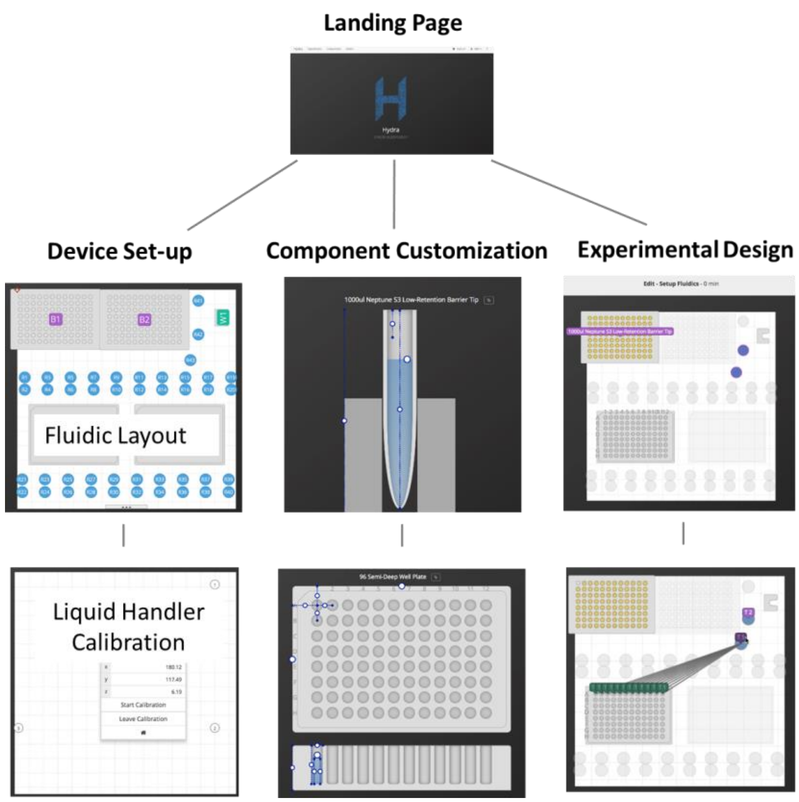

Supplementary Figure ~~S2~~S3. Hydra software screen shots highlighting key features of device setup, component customization, and experimental design. All Interrogator programming is performed using this graphical Hydra software interface.

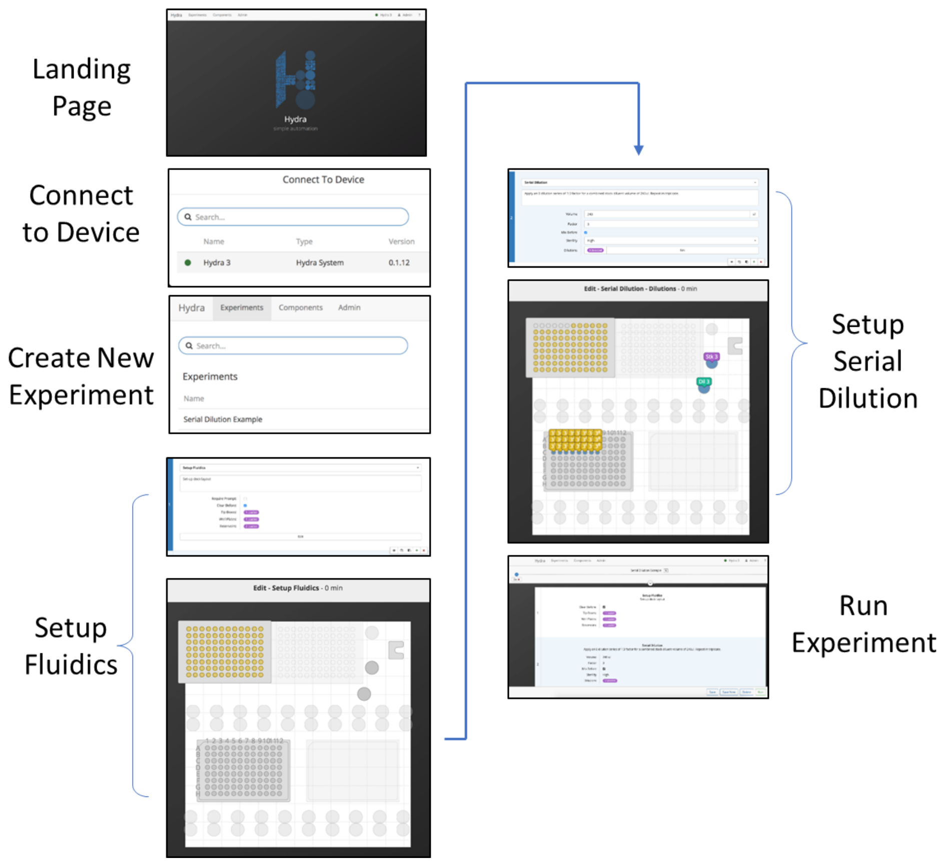

Supplementary Figure ~~S3~~S4. Hydra software screen shots of the rapid workflow involved in designing and executing a typical experiment

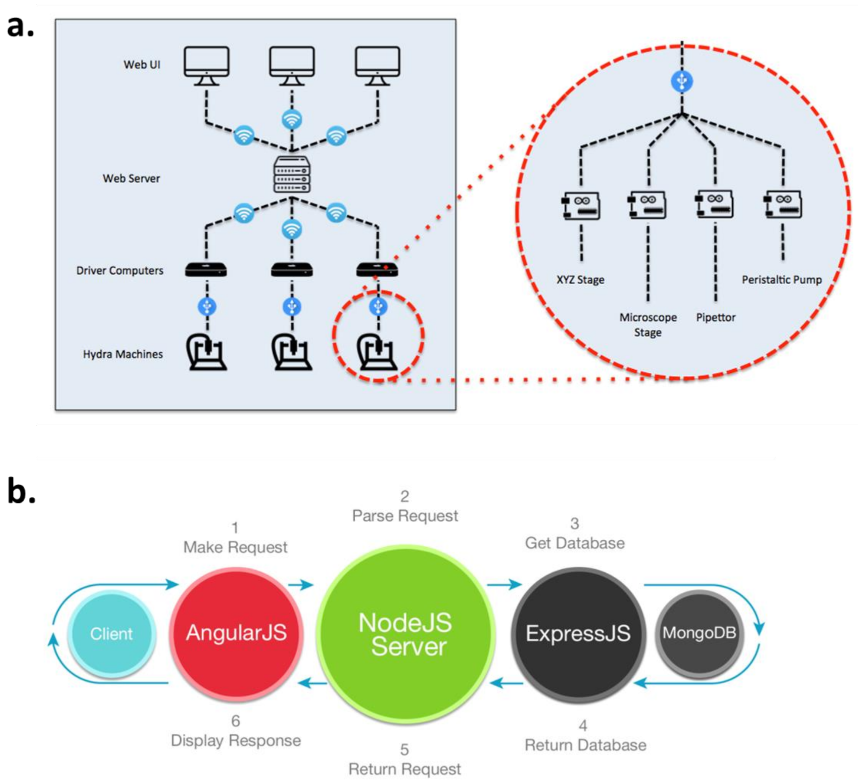

Supplementary Figure ~~S4~~S5. Schematic of Hydra **(A)** system communication structure and **(B)** network software architecture.

Formatted: Font: Bold

Formatted: Font: Bold

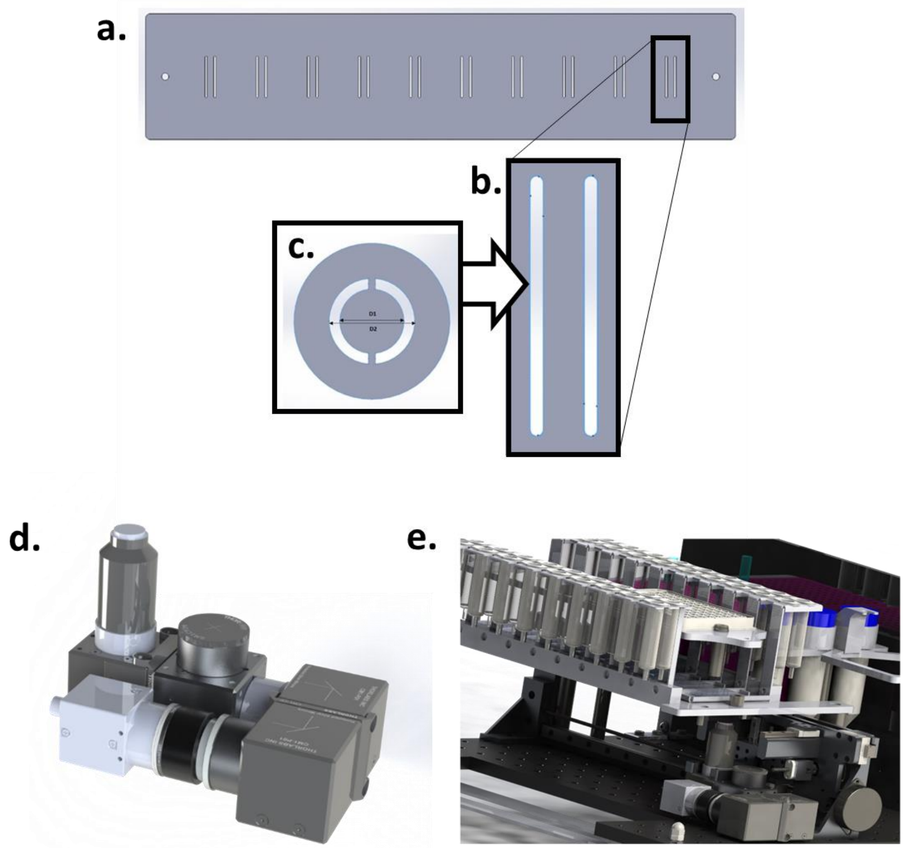

Supplementary Figure ~~S5~~S6. Rendering of the phase plate (**A**) used to generate phase contrast-like illumination in Organ Chips while enabling scanning across their channel length. Each Organ Chip cartridge location is directly below each phase slot feature (**B**), which was designed based on standard condenser phase ring geometry (**C**). An epifluorescence module (**D**) was designed to enable fluorescence imaging in the Interrogator (**E**).

Formatted: Font: Bold

Formatted: Font: Bold

Formatted: Font: Bold

Formatted: Font: Bold

Formatted: Font: Bold

129

130

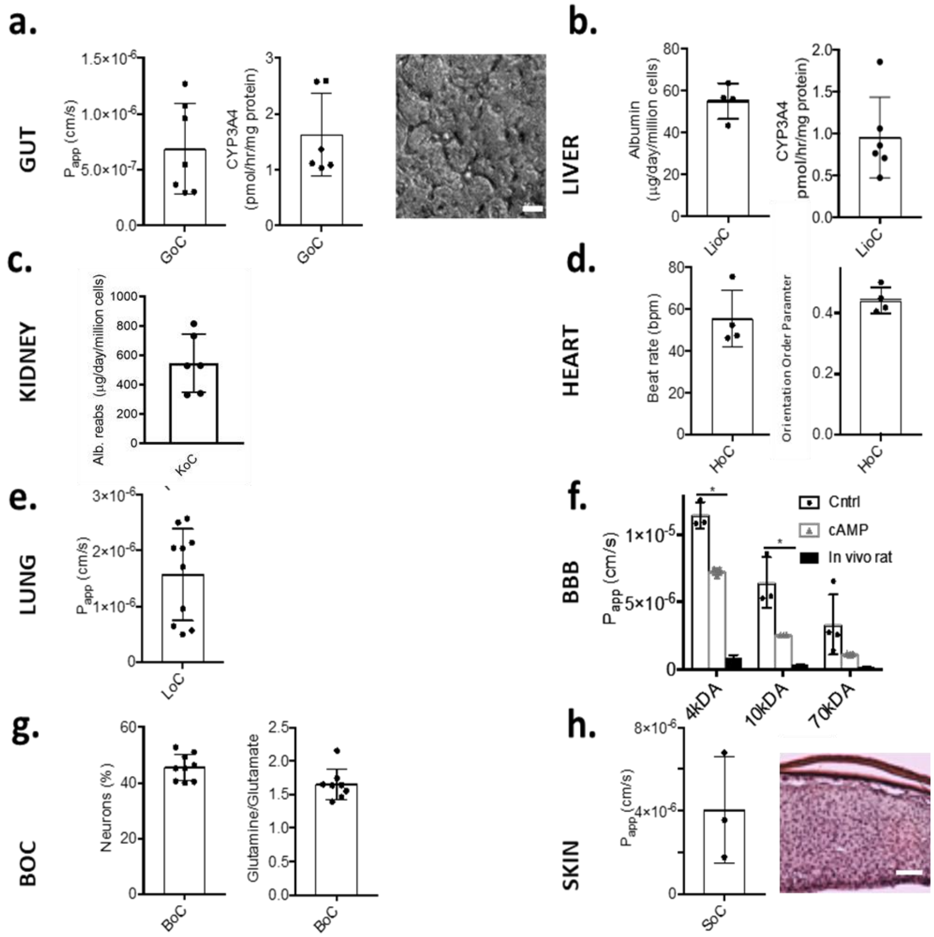
a.
GUT
P_{app} (cm/s)
1.5×10-6
1.0×10-6
5.0×10-7
0.0
GoC
CYP3A4 (pmol/hr/mg protein)
GoC
b.
LIVER
Albumin (μg/day/million cells)
LioC
CYP3A4 pmol/hr/mg protein)
LioC
c.
KIDNEY
Alb. reabs (μg/day/million cells)
KoC
d.
HEART
Beat rate (bpm)
HoC
Orientation Order Paramter
HoC
e.
LUNG
P_{app} (cm/s)
3×10-6
2×10-6
1×10-6
LoC
f.
BBB
P_{app} (cm/s)
1×10-5
5×10-6
Cntrl
cAMP
In vivo rat
4kDA
10kDA
70kDA
g.
BOC
Neurons (%)
BoC
Glutamine/Glutamate
BoC
h.
SKIN
P_{app} (cm/s)
8×10-6
4×10-6
SoC

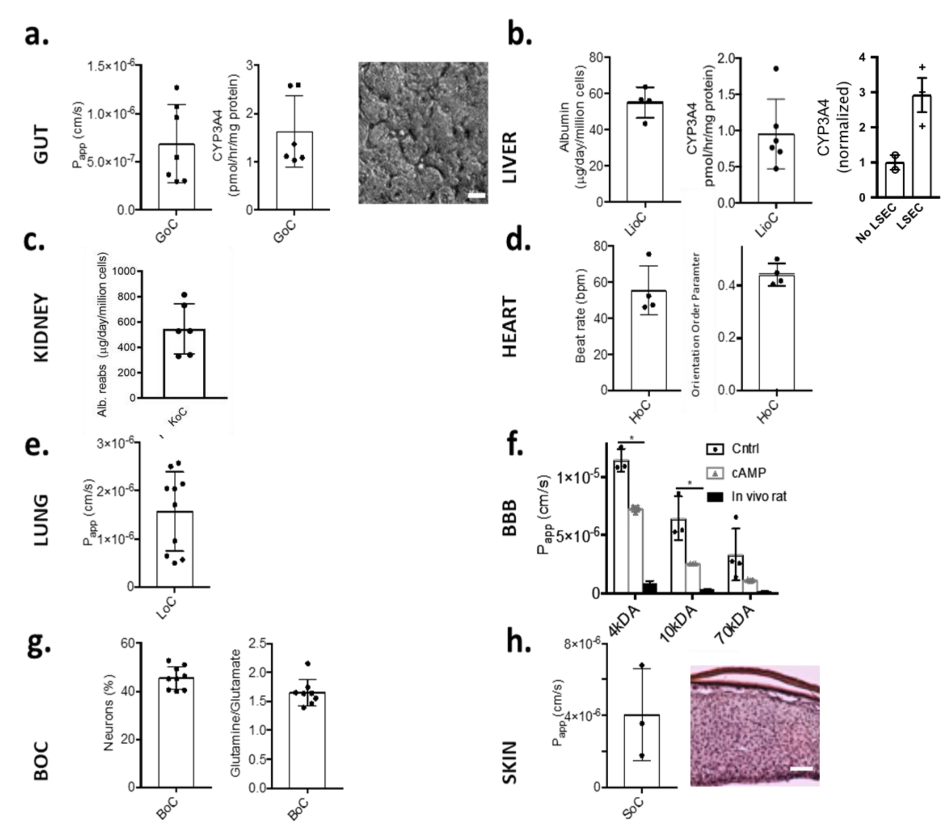

Supplementary Figure ~~S6~~S7. Organ Chip-specific readouts prior to linking demonstrating organ maturity. **(A)** Gut Chip: Cascade blue® (596 Da) permeability, n=7, CYP3A4 activity, and bright field imaging of villi, scale 50 μm. **(B)** Liver Chip: albumin production and CYP3A4 activity, n=4 and n=6, influence of liver endothelial cells on Liver Chip function, n=2 **(C)** Kidney Chip: albumin reabsorption, n=3 **(D)** Heart Chip: beat rate and orientation order parameter (OOP[11]), n=4 **(E)** Lung Chip: Texas Red^{TM} (3 kDa) permeability, n=10 **(F)** BBB Chip permeability effect of Cyclic adenosine monophosphate (cAMP) and comparison to rat *in vivo* data : Inulin-FITC (2-5 kDa, listed as 4 kDa for comparison with literature *in vivo* data) p=0.002, n=3, Dextran-Cascade blue® (10 kDa) p= 0.024, n=3, Dextran-Texas Red^{TM} (70 kDa) permeability, n=4, *in vivo* data[12] **(G)** Brain Chip: ratio of neuronal cells and glutamine:glutamate ratio, n=9 and n=8 **(H)** Skin Chip: Cascade Blue (596Da) permeability, n=3 at left and H&E stained section through chip showing squamous epidermis overlying a thick epidermis (bar, 50 μm).

Formatted: Font: Bold
Formatted: Font: Bold
Formatted: Font: Bold
Formatted: Font: Bold
Formatted: Font: Bold
Formatted: Font: Bold
Formatted: Font: Bold
Formatted: Font: Bold
Formatted: Font: Symbol

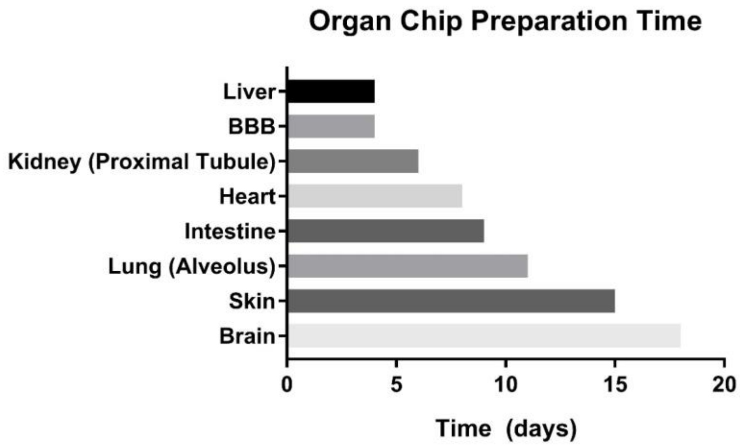

Supplementary Figure S8~~7~~. Length of culture time required for Organ Chips to reach a mature morphological and functional state. After the indicated time the Organ Chips were used for linkage experiments.

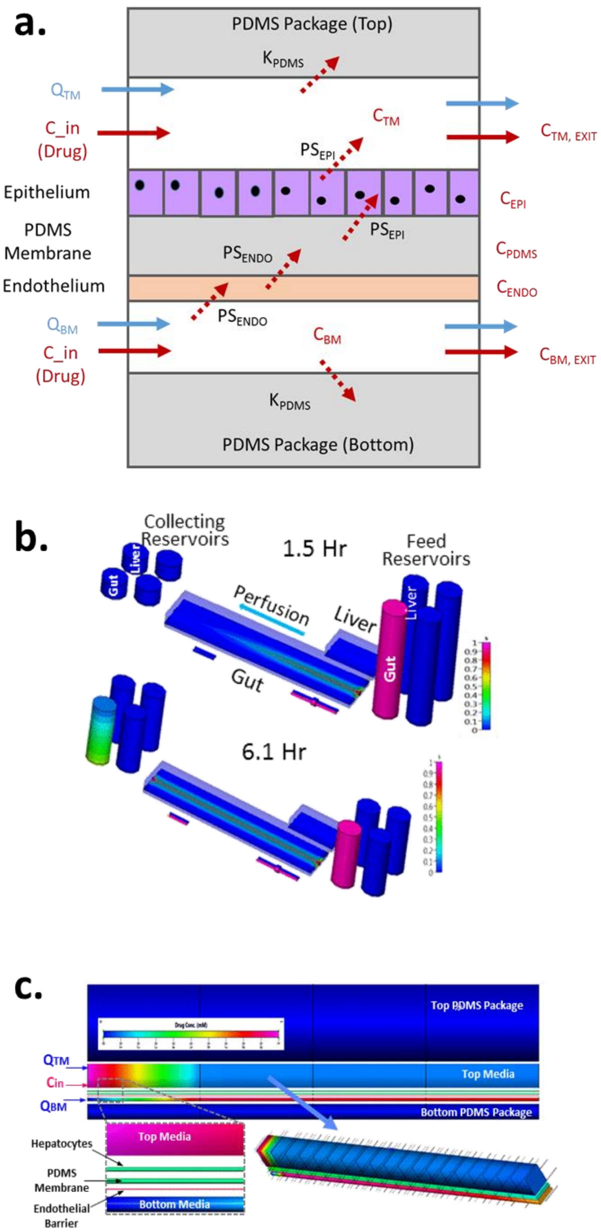
a.
PDMS Package (Top)
K_PDMS
Q_TM
C_in (Drug)
C_TM
C_TM, EXIT
PS_EPI
Epithelium
C_EPI
PDMS Membrane
PS_ENDO
C_PDMS
Endothelium
C_ENDO
Q_BM
C_BM
C_BM, EXIT
PDMS Package (Bottom)
b.
Collecting Reservoirs
1.5 Hr
Feed Reservoirs
Gut
Liver
Perfusion
6.1 Hr
c.
Top PDMS Package
Top Media
Bottom PDMS Package
QTM
Cin
QBM
Hepatocytes
PDMS Membrane
Endothelial Barrier
Bottom Media

Supplementary Figure S9~~8~~. Computational Microphysiological Model of a generic Organ Chip **(A)**. Each Organ Chip model is spatially resolved in both stream-wise and cross-stream direction (top PDMS, top channel media, epithelial cell layer, membrane, endothelial cell layer, bottom channel media, bottom PDMS). **(B)** A quantitative reduced order 3D model (Q3D) enables tracking drug dynamics through linked Organ Chips (Gut to Liver shown here). Two time instances show initial transport of the gut microchannel at 1.5 hr and at 6.1hr. The media from “vascular” collecting reservoirs is periodically transferred to downstream linked Organ Chips using the Interrogator. **(C)** Detailed view of the 3D spatially resolved Organ Chip model showing the geometrical/mesh resolution in the cross-stream and stream-wise (axial) directions.

Formatted: Font: Bold

Formatted: Font: Bold

Formatted: Font: Bold

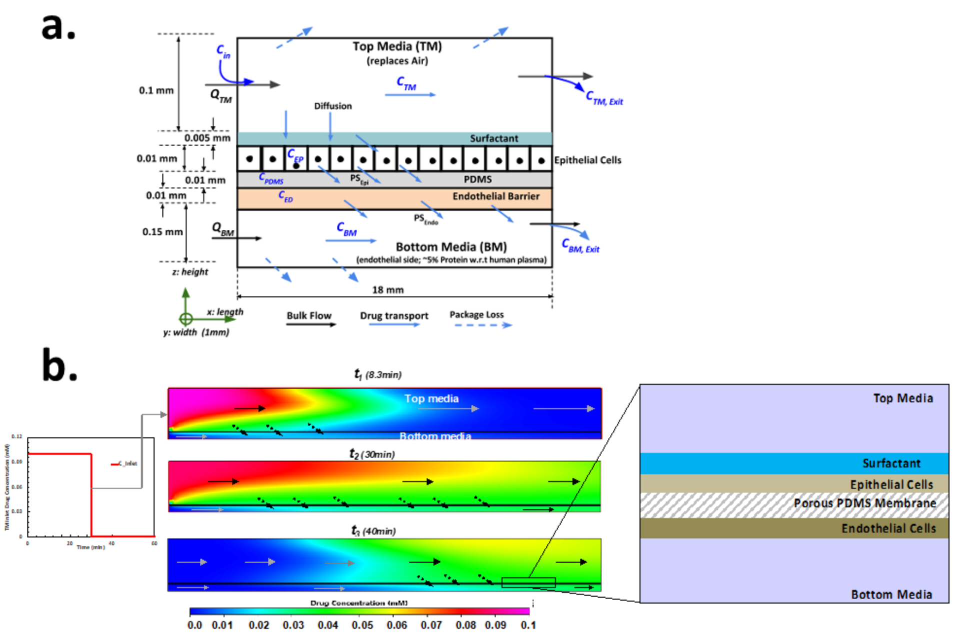

Supplementary Figure S~~9~~10. Computational Model of the Lung Chip **(A)** Reduced-Order Model of Lung Chip in liquid-liquid interface culture, 4 compartments in axial direction, **(B)** High-Fidelity Model of drug bolus movement and apical→basal mass transfer through Lung Chip membrane over time.

Formatted: Font: Bold

Formatted: Font: Bold

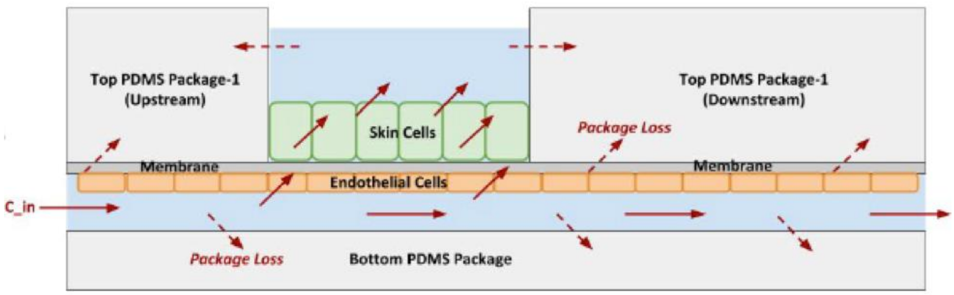

Supplementary Figure S11~~0~~. Computational Model of the Skin Chip: Reduced-Order Model of Skin Chip, 4 compartments in axial direction

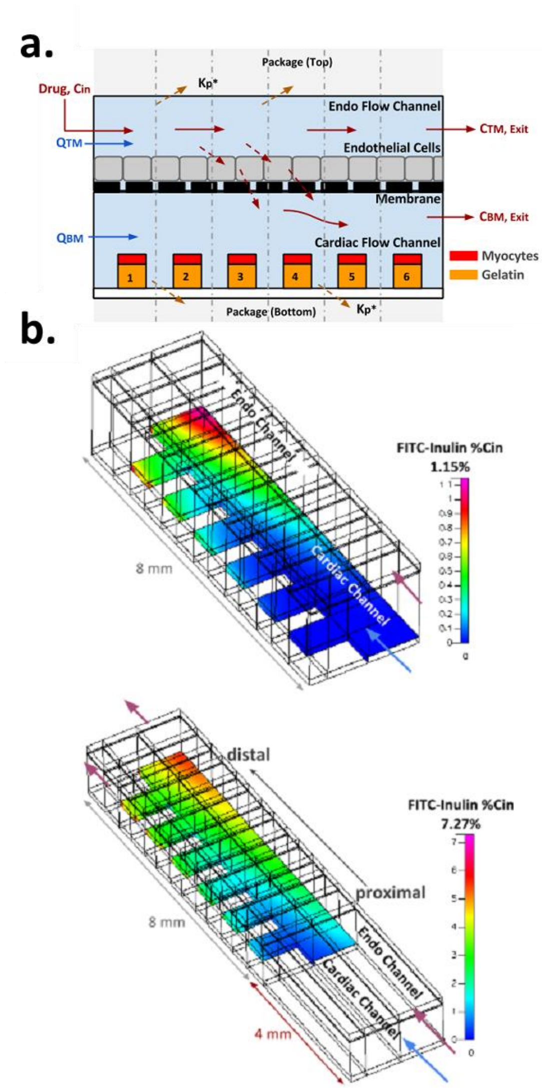

Supplementary Figure S12~~1~~. Computational model of the Heart Chip **(A)** Reduced-Order Model of MTF Heart Chip (6 compartments in axial direction), **(B)** High-fidelity models of MTF Heart Chip predict increased apical→basolateral mass transfer of high MW tracer when increasing chip length from 8 mm (top) to 12 mm (bottom).

Formatted: Font: Bold

Formatted: Font: Bold

a.

Parameter	Value	Unit
Step Pulse	10	µs
Step Idle Delay	100	ms
Step Size (X & Y, Z)	20.051, 200.000	step/mm
Max Velocity (X & Y, Z)	200, 56	mm/s
Acceleration (X & Y, Z)	400, 160	mm/s^2
Motion Envelope (X & Y, Z)	310, 135	mm

b.

```
$0=10 (step pulse, usec)
$1=100 (step idle delay, msec)
$2=0 (step port invert mask:00000000)
$3=3 (dir port invert mask:00000011)
$4=0 (step enable invert, bool)
$5=1 (limit pins invert, bool)
$6=0 (probe pin invert, bool)
$10=1 (status report mask:00000001)
$11=0.020 (junction deviation, mm)
$12=0.010 (arc tolerance, mm)
$13=0 (report inches, bool)
$20=1 (soft limits, bool)
$21=1 (hard limits, bool)
$22=1 (homing cycle, bool)
$23=7 (homing dir invert mask:00000111)
$24=60.000 (homing feed, mm/min)
$25=2000.000 (homing seek, mm/min)
$26=100 (homing debounce, msec)
$27=1.000 (homing pull-off, mm)
$100=20.051 (x, step/mm)
$101=20.051 (y, step/mm)
$102=200.000 (z, step/mm)
$110=12000.000 (x max rate, mm/min)
$111=12000.000 (y max rate, mm/min)
$112=3400.000 (z max rate, mm/min)
$120=400.000 (x accel, mm/sec^2)
$121=400.000 (y accel, mm/sec^2)
$122=160.000 (z accel, mm/sec^2)
$130=310.000 (x max travel, mm)
$131=310.000 (y max travel, mm)
$132=135.000 (z max travel, mm)
```

Supplementary Figure S13~~2~~. Motion system parameters **(A)** and ~~GRBL~~ stepper motor control ~~shield~~ settings **(B)** that define the characteristic behavior of the system.

Formatted: Font: Bold

Formatted: Font: Bold

Supplementary Movies

SI Movie 1

Overview of Interrogator system components and Organ Chip linking.

SI Movie 2

Microscope module movie of gut chip stretching.

SI Movie 3

Heart Chip beating after being linked for 3 weeks on the Interrogator platform.

SI Movie 4

High-fidelity diffusion model of the Heart Chip.

SI Movie 5

CoBi Q-3D Model of Gut-Liver Chip Linking